Single-Nanowire Raman Microprobe Studies of Doping-, Temperature-, and Voltage-Induced Metal–Insulator Transitions of $W_xV_{1-x}O_2$ Nanowires

Luisa Whittaker,[†,§] Tai-Lung Wu,[‡,§] Adam Stabile,[‡] G. Sambandamurthy,[‡,*] and Sarbajit Banerjee[†,*]

[†]Department of Chemistry and [‡]Department of Physics, University at Buffalo, The State University of New York, Buffalo, New York 14260, United States.
[§]These authors contributed equally to this work.

ABSTRACT Considerable recent research interest has focused on mapping the structural phase diagrams of anisotropic VO_2 nanobeams as model systems for elucidating single-domain behavior within strongly correlated electronic materials, to examine in particular the coupling of lattice and orbital degrees of freedom. Nevertheless, the role of substitutional doping in altering the phase stabilities of competing ground states of VO_2 remains underexplored. In this study, we use individual nanowire Raman microprobe mapping to examine the structural phase progressions underlying the metal–insulator transitions of solution-grown $W_xV_{1-x}O_2$ nanowires. The structural phase progressions have been monitored for three distinctive modes of inducing the electronic metal–insulator phase transition: as a function of (a) W doping at constant temperature, (b) varying temperature for specific W dopant concentrations, and (c) varying applied voltage for specific W dopant concentrations. Our results suggest the establishment of a coexistence regime within individual nanowires wherein M1 and R phases simultaneously exist before the percolation threshold is reached and the nanowire becomes entirely metallic. Such a coexistence regime has been found to exist during both temperature- and voltage-induced transitions. No evidence of an M2 phase is observed upon inducing the electronic phase transition by any of the three distinctive methods (temperature, doping, and applied voltage), suggesting that substitutional tungsten doping stabilizes the M1 phase over its M2 counterpart and further corroborating that the latter phase is not required to mediate M1→R transformations.

KEYWORDS: nanowires · phase transitions · VO_2 · solid solutions · doping · Raman spectroscopy

Tweaking the intricately entangled lattice, orbital, and spin degrees of freedom in strongly correlated electronic materials has emerged as a validated tool for discovery of regions of phase space characterized by exotic spin and transport behavior and for manifestation of physical phenomena characterized by unprecedented complexity.[1−3] Scaling strongly correlated electronic materials to nanoscale dimensions, below the intrinsic domain size, represents a possible alternative for examining materials close to the single-domain limit.[4] As a canonical example of a material exhibiting electronic instabilities, the metal–insulator transitions of VO_2 have attracted much recent scrutiny.[3−7] The impressive magnitude of the phase transition, its proximity to room temperature, and the intrinsic <100 fs time scale portend applications in electrostatically mediated Mott field-effect transistors, gas sensors with distinctive threshold voltages for induction of the metal–insulator transition, strain sensors, infrared polarizers and waveguides, and thermochromic coatings, among other applications.[4,8−11] VO_2 nanobeams grown by physical vapor transport of granular VO_2 material onto substrates held at high temperatures within hot wall furnaces[12] have emerged as among the most popular model systems for exploration of finite size effects in this material and have been used to experimentally map an expansive region of the multidimensional strain–temperature structural and electronic phase space.[7,11,13,14] An important caveat that has emerged from these studies is that geometric confinement and inhomogeneous strain coupling in anisotropic nanostructures renders the phase space substantially more complex than naively expected from a single-domain perspective. Solution-grown VO_2 nanostructures are relatively underexplored but represent an attractive alternative since they can be readily dispersed onto any substrate and the synthetic parameters can be facilely tuned to accommodate substitutional dopants.[8,15] A prominent gap in our knowledge of these systems is the precise role of substitutional doping, which is ubiquitously used in the bulk to manipulate the electronic phase diagram but has scarcely been examined for materials with reduced dimensionality.

* Address correspondence to sg82@buffalo.edu, sb244@buffalo.edu.

Received for review August 8, 2011 and accepted October 6, 2011.

Published online October 11, 2011
10.1021/nn203542c

Here, we present a single-nanowire Raman microprobe study of metal−insulator transitions of $W_xV_{1-x}O_2$ nanowires induced separately by doping, temperature, and applied voltage.[4,16,17] Examining the phase transitions of individual nanowires allows us to derive an intrinsic structural phase diagram, examine the role of substitutional tungsten doping, and address the (absent) intermediacy of the M2 phase.

The metal−insulator transition in VO_2 is accompanied by the structural phase transition of a Jahn−Teller distorted tetragonal rutile (R) phase to a lower-symmetry monoclinic M1 phase wherein adjacent pairs of VO_6 octahedra along the tetragonal *c* axis are dimerized and tilted to form a zigzag chain (reconstructed as the crystallographic *a* axis of the M1 phase).[4] In vapor-transport-grown VO_2 nanobeams strongly coupled to the underlying substrate, Park and co-workers demonstrated the striking coexistence and quasi-periodic organization of metallic and insulating domains, visible even in optical microscopy images, resulting from a balance between minimization of strain energy of the coupled nanobeam/substrate system and the domain wall energies developed at the boundaries of the insulating/metallic domains.[18] Other researchers were able to use Raman microprobe analysis and micro-X-ray diffraction to surmise the presence of a different monoclinic polymorph, the M2 phase, within substrate-coupled nanobeams with increased tensile strain thought to play an important role in stabilization of this polymorph.[19,20] The M2 phase can be visualized as comprising two interpenetrating networks of the M1 and R phases, wherein alternate chains of VO_6 octahedra along the tetragonal *c* axis are either dimerized but not tilted or tilted in a zigzag manner but not dimerized.[4,21,22] In the bulk, this phase is stabilized by uniaxial strain or *via* doping with Cr^{3+} or Al^{3+} on the cation sublattice.[22,23] Despite initial conjectures regarding the universal intermediacy of the M2 phase for mediating the M1→R transition and the role of finite size in coaxing the system toward this metastability, it is now clear that the observation of this polymorph during the metal−insulator transitions of VO_2 nanobeams is primarily a consequence of the inhomogeneous strain fields generated due to coupling of the nanobeams to the substrate.[7,11,13,14,24] For unconstrained granular samples of VO_2, Corr *et al.* have demonstrated using a comprehensive total scattering analysis that while there is a distinctive phase coexistence regime for the M1 and R phases, the pair distribution functions can be accounted for using exclusively these two phases without needing to invoke the presence of the M2 polymorph.[25] In this context, Donev and co-workers have performed single-nanoparticle Raman microprobe analysis on VO_2 nanoparticles fabricated by a combination of focused ion beam lithography and pulsed laser deposition. The individual nanoparticles with precisely controlled stoichiometry are observed to hysteretically switch between M1 and R phases without any evidence for intermediacy of the M2 phase.[26] Tselev *et al.* have recently performed an elegant Ginzburg−Landau analysis of the structural phase transformations at the VO_2 metal−insulator transition and have noted that transitions from the rutile to the M1 and M2 phases are originated at the same special point in the Brillouin zone of the rutile lattice.[24] Consequently, both the monoclinic polymorphs can be thought of as equivalent routes to resolve the instability of the tetragonal rutile phase at the phase transition temperature with minor perturbations such as to local strain tensors determining the more energetically favorable transformation induced at the zone boundary.[24] These researchers have thus discounted the possibility of the M2 phase playing a role as an intermediate between the M1 and R phases. In a recent article, Lauhon and co-workers have emphasized the importance of not just external strain and substrate coupling but also precise stoichiometry gradients and electron/hole doping in establishing inhomogeneous internal strain and inducing localized perturbations that result in distinctive rutile domains being stabilized within VO_2 nanobeams down to temperatures as low as 103 K.[27] M2 phases are observed to be stabilized in nanobeams exposed to more oxidizing atmospheres, consistent with generation of V^{5+} sites and analogous to the situation with Cr^{3+} doping.[27]

Hydrothermally prepared free-standing VO_2 nanostructures present an intriguing counterpoint to the vapor-transport-synthesized VO_2 nanobeams noted above since they can be solvent cast onto different substrates and can further be substitutionally doped to varying extents by the incorporation of the appropriate precursors. We present the first individual nanowire Raman measurements of these solution-grown nanostructures. The tunability of substitutional tungsten incorporation in $W_xV_{1-x}O_2$ nanowires permits evaluation of the distinctive role of tungsten doping in altering the phase stabilities of the nanostructures. Thermal and voltage-induced phase transitions are also separately examined by Raman microprobe measurements.

RESULTS AND DISCUSSION

In previous work, we have been able to use finite size in conjunction with substitutional tungsten doping to depress the phase transition temperature of $W_xV_{1-x}O_2$ nanowires down to −20 °C as measured by ensemble differential scanning calorimetry and single-nanowire electrical transport measurements.[4,16,17] Furthermore, the depression in the critical phase transition temperatures upon tungsten doping far surpasses corresponding values for bulk $W_xV_{1-x}O_2$ of the same composition, suggesting substantial alteration of the phase diagram

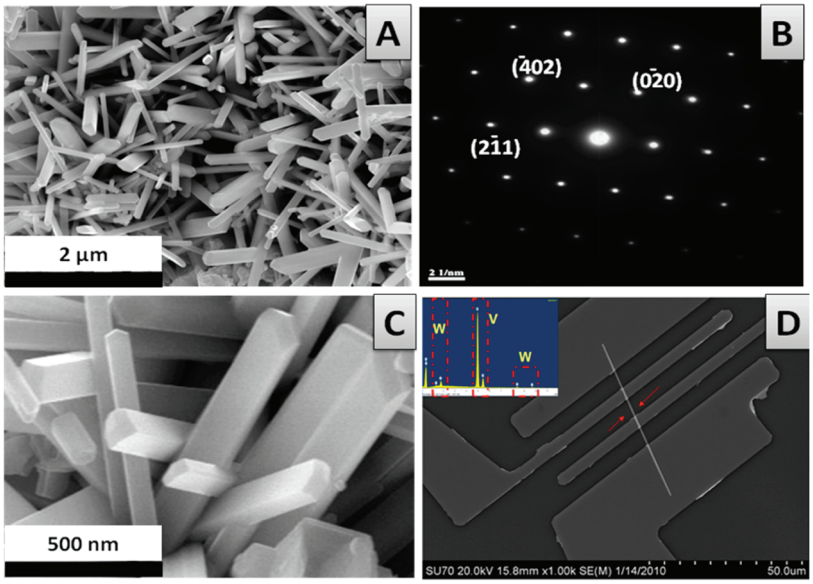

Figure 1. (A) SEM image of W-doped VO_2 nanowires with a nominal W concentration of 0.4 atom %. (B) SAED pattern acquired for a single $W_xV_{1-x}O_2$ nanowire, indexed to the M1 phase. (C) Cross-sectional SEM image indicating the approximately rectangular cross sections of the nanowires. (D) SEM image of an individual $W_xV_{1-x}O_2$ nanowire with $x \sim 0.40$ atom % aligned across four electrodes. The device has been fabricated on a Si/SiO_2 (300 nm) substrate after solution casting the nanowires. The inset shows an energy-dispersive X-ray spectrum acquired for the nanowire.

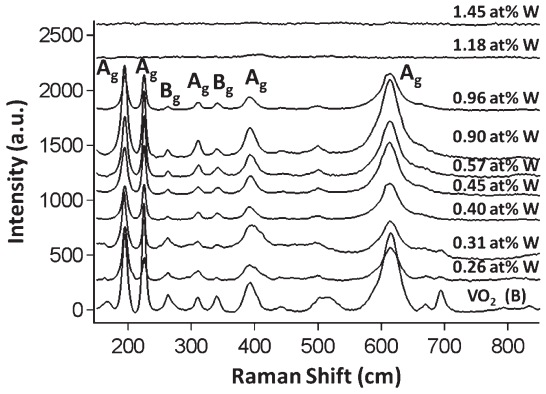

Figure 2. Room-temperature Raman spectra acquired for $W_xV_{1-x}O_2$ nanowires with increasing tungsten doping. The M1 phase is discernible up to 0.96 atom % W doping, whereas the rutile phase is surmised from the absence of Raman bands beyond 1.18 atom % W doping. Characteristic modes of the M2 phase are not observed in any of the samples.

as a consequence of finite size. The marked deviations from bulk behavior are rationalized in terms of a percolative model of the phase transition wherein cooperative avalanche processes facilitate the insulator→metal transition, establishing a percolating metallic path for transport, but tend to impede the reverse metal→insulator transition resulting in supercooling of the metallic phase.

Figure 1 shows overview and cross-sectional SEM images and a SAED pattern for W-doped VO_2 nanowires. The nanowires have rectangular cross sections with widths ranging from 30 to 300 nm but considerably thinner vertical dimensions (heights).[16] The SAED pattern in Figure 1B is constant along the length of the nanowires, suggesting the single-crystalline nature of the nanowires. Figure 1D depicts a single nanowire aligned within a device geometry such as used for voltage-driven experiments.

Metal−Insulator Transition at Constant Temperature as a Function of Varying W Doping. Figure 2 depicts ensemble room-temperature (298 K) Raman spectra acquired for $W_xV_{1-x}O_2$ nanowires with increasing tungsten doping. The space groups for the R and M1 phases are $P4_2/mnm$ (D_{4h}^{14}) and $P2_1/C$ (C_{2h}^{3}), respectively, and the pronounced differences in local symmetry give rise to distinctive Raman signatures (the M2 phase crystallizes in the C_{2h}^{5} space group and also has distinctive Raman modes).[13,28] By group theory analysis, the M1 phase is characterized by 18 Raman-allowed modes, 9 with A_g symmetry and 9 with B_g symmetry. The mode assignments noted in Figure 2 are based on previously reported polarized Raman studies and group theory predictions.[13,28,29] We evidence small shifts of the prominent 189 and 607 cm^{-1} A_g modes to 194 and 611 cm^{-1}, respectively, originating from the incorporation of substitutional tungsten dopants. Conversely, the R phase is characterized by a broad featureless luminescence.[13,19,27,29] Figure 2 illustrates that at 1.18 atom % W doping and beyond, the prominent Raman signals of the M1 phase disappear, corroborating the stabilization of the metallic R phase at room temperature.[16] We have noted in previous work that tungsten doping of nanowires induces a depression in phase transition temperatures far exceeding the 23−26 °C/atom % W norm established for bulk materials and VO_2 thin films.[16] No evidence for formation of the M2 phase (characterized by splitting of the

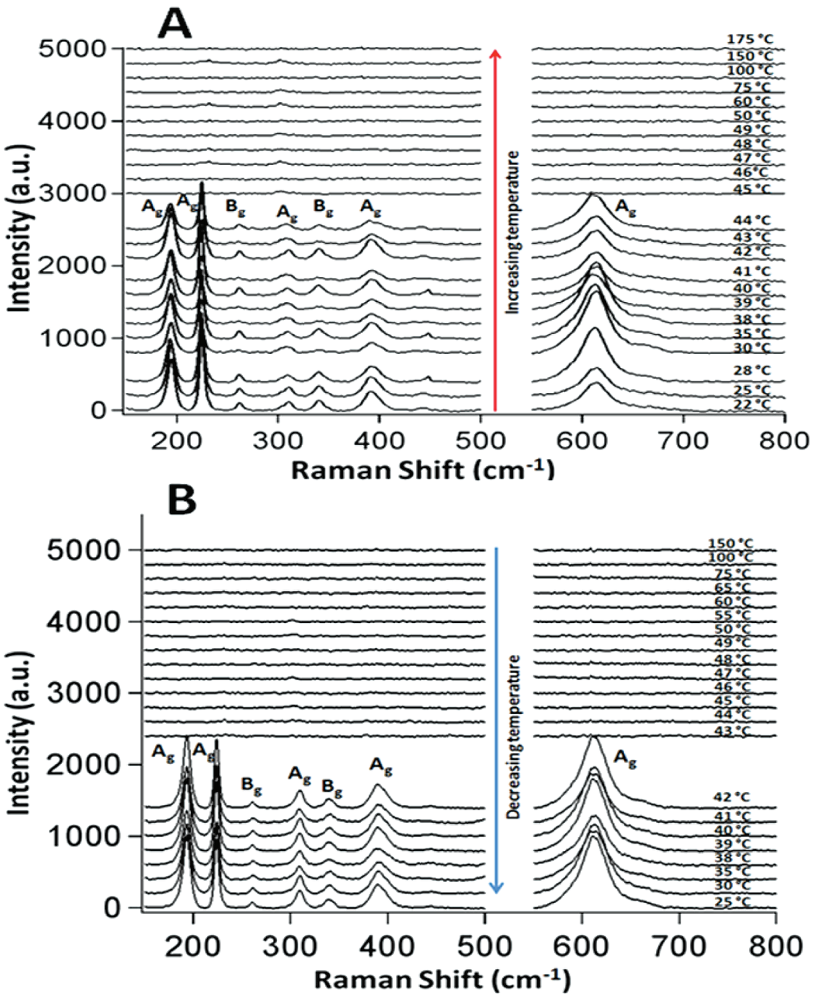

Figure 3. Raman spectra acquired for an individual $W_xV_{1-x}O_2$ nanowire with $x \sim 0.4$ atom % as a function of increasing and decreasing temperature.

221 cm^{-1} A_g mode and shift of the 607 cm^{-1} mode to 649 cm^{-1}) is observed at any of the tungsten doping concentrations.

Metal–Insulator Transition for Specific W Doping Concentrations as a Function of Temperature. Raman spectra have been acquired across the metal–insulator transition for a single $W_xV_{1-x}O_2$ nanowire with a nominal W doping of $x \sim 0.40$ atom %. Figure 3 depicts that, at low temperatures, the nanowire clearly exhibits Raman signatures of the M1 phase. Upon heating, between 44 and 45 °C, the nanowire abruptly and discontinuously switches to the R phase and the characteristic Raman bands of the M1 phase are completely lost. No major diminution in intensity or shifts of the M1 Raman modes are observed leading up to the phase transition, suggesting nucleation of the R phase and a discontinuous jump of the domain wall without intermediacy of triclinic (T) or M2 phases. The abruptness of the change in spectral signatures suggests that the phase transition is manifested across a large volume without a substantial coexistence regime for these nanowires, although a short-lived coexistence regime cannot be ruled out.[24] The direct M1→R transition without intermediacy of M2 or T phases likely captures the intrinsic phase diagram of $W_xV_{1-x}O_2$ as a result of substitutional doping (as also seen by doping-induced transition evidenced in Figure 2). Identical abrupt M1→R transition behavior has also been observed for $W_{0.004}V_{0.996}O_2$ nanowires on Ta substrates, corroborating the idea that these nanowires are not substantially strained. Since the nanowires are cast onto the substrates by solution casting from 2-propanol, considerable slip between the nanowire and the substrate during the heating process is expected, which relaxes tensile stresses generated due to the differential thermal expansion coefficients of VO_2 and the SiO_2 substrate. As noted above, a direct M1→R transition has also been noted for stoichiometric VO_2 nanobeams that are unconstrained or reside on compliant substrates.[14,24] An analogous abrupt R→M1 transition is evidenced during cooling with a slight hysteresis (Figure 3B).

In Figure 4, we follow the phase transformation of a nanowire with a nominal composition of $W_{0.009}V_{0.991}O_2$ wherein the metal–insulator transition has been

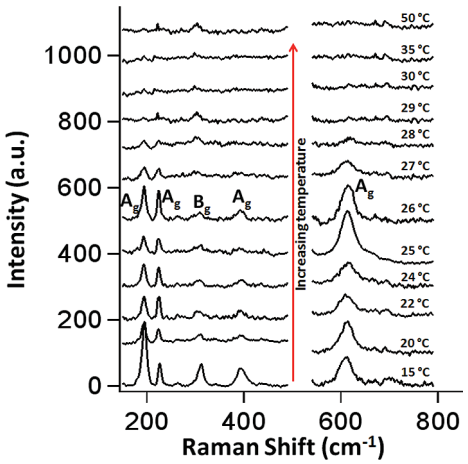

Figure 4. Raman spectra acquired for an individual $W_xV_{1-x}O_2$ nanowire with $x \sim 0.9$ atom % as a function of increasing temperature.

depressed in proximity to room temperature. Upon heating from 15 °C, the spectral signatures of the M1 phase are distinctly retained without significant change in intensity up to 26 °C. Subsequently, a pronounced diminution of M1 Raman bands is evidenced with further heating at 27 and 28 °C, and the bands are no longer discernible above the baseline at 29 °C. The diminished intensity of the M1 Raman modes suggests the nucleation of the metallic R phase and a coexistence regime spanning 26−29 °C, suggesting a phase progression of M1→ M1+R→R, as has also been noted in bulk studies of unconstrained VO_2 or granular VO_2 thin films.[6,25] No discernible peak shifts or peak splitting are noted for the 611 and 225 cm^{-1} A_g modes, again ruling out the intermediacy of the M2 phase.

Metal−Insulator Transition for Specific W Doping Concentrations as a Function of Applied Voltage. We next turn our attention to examining the structural phase transformations accompanying the voltage-induced metal−insulator transition in $W_xV_{1-x}O_2$ nanowires. These measurements have been acquired for nanowires aligned within device geometries such as illustrated in Figure 1D. The nanowires can thus be thought to be clamped onto the substrate by the deposited electrodes. The inset to Figure 5A shows a resistance *versus* temperature plot of a nanowire with the same nominal tungsten doping, $x \sim 0.4$, as examined in Figure 3. The nanowire is seen to be completely metallic by 50 °C, which is similar to the phase transformation behavior noted in Figure 3 accounting for experimental error and the clamped *versus* unconstrained nature of the two experiments. Figure 5A further indicates a current *versus* voltage plot measured at −20 °C, suggesting a sharp threshold voltage beyond which the current discontinuously rises as the nanowire transforms to a metallic state. The dotted vertical lines correspond to voltages at which Raman spectra have been acquired, as depicted in Figure 5B. In the absence of a voltage or at low applied voltages, prominent Raman modes ascribed to the M1 phase are discernible up to 0.60 V. At 0.61 V, the 625 cm^{-1} mode is slightly upshifted and broadened as well as diminished in intensity, suggesting a distorted M1 phase and the nucleation of R domains as the current starts to increase (Figure 5A). At 0.62 V and beyond, the R phase appears to be the preponderant phase; no evidence of the M2 phase is observed even for these clamped 1D nanowires. Interestingly, at 0.62 V, the Raman spectrum in Figure 5B shows the R phase to be dominant, but from the transport data in Figure 5A, the nanowire has yet to reach a completely metallic state, likely because complete percolation of metallic domains has not yet been achieved. Notably, almost 80% of the volume of the nanowire is required to be in the metallic R phase before metallic transport can be achieved in this 1D system (in comparison to only 16% required for percolation in a 3D object).[20] At voltages slightly higher than 0.62 V, which is very near the threshold voltage, the nanowires abruptly switch to the metallic state even from the slight laser heating that results from acquiring the Raman spectrum over 300 s. At 0.70 V, the M1 phase is no longer discernible and the nanowire is also completely metallic. The data here again suggest a phase progression of M1→M1+R→R with a distinctive coexistence regime wherein the percolation threshold has yet to be reached. Remarkably, the small upshift in the 611 cm^{-1} mode suggests some distortions to the M1 phase (likely at the M1/R domain wall), but no M2 phase is evidenced even though the nanowires here are clamped and thus subject to greater strain.

The absence of the M2 phase in our measurements provides intriguing insight into the intrinsic phase diagram of W-doped VO_2. As Tselev *et al.* have suggested, the M1 and M2 phases are simply two ways to resolve the instability of the R lattice below the phase transition temperature.[24] Minor perturbations to the free energy functional, such as through manipulation of the strain tensors or *via* the application of chemical pressure through doping, can make one phase more thermodynamically favorable than the other. Doping with Cr^{3+} and Al^{3+} is known to stabilize the M2 phase, primarily due to the role of these dopants in generating V^{5+} species and the concomitant hole doping.[22,23] In contrast, doping with W^{6+} adds two electrons to the VO_2 band structure, creating V^{3+} sites and disrupting V^{4+}−V^{4+} dimerization, and thus likely stabilizes the M1 phase with respect to its M2 counterpart. Such preferential stabilization of the M1 phase has also been alluded to for undoped VO_2 nanostructures with high oxygen vacancy concentrations.[27] Clearly, even the presence of strain in clamped $W_xV_{1-x}O_2$ nanowires is not able to offset the preferential stabilization of the M1 phase, and the phase progression remains M1→M1+R→R for these materials.

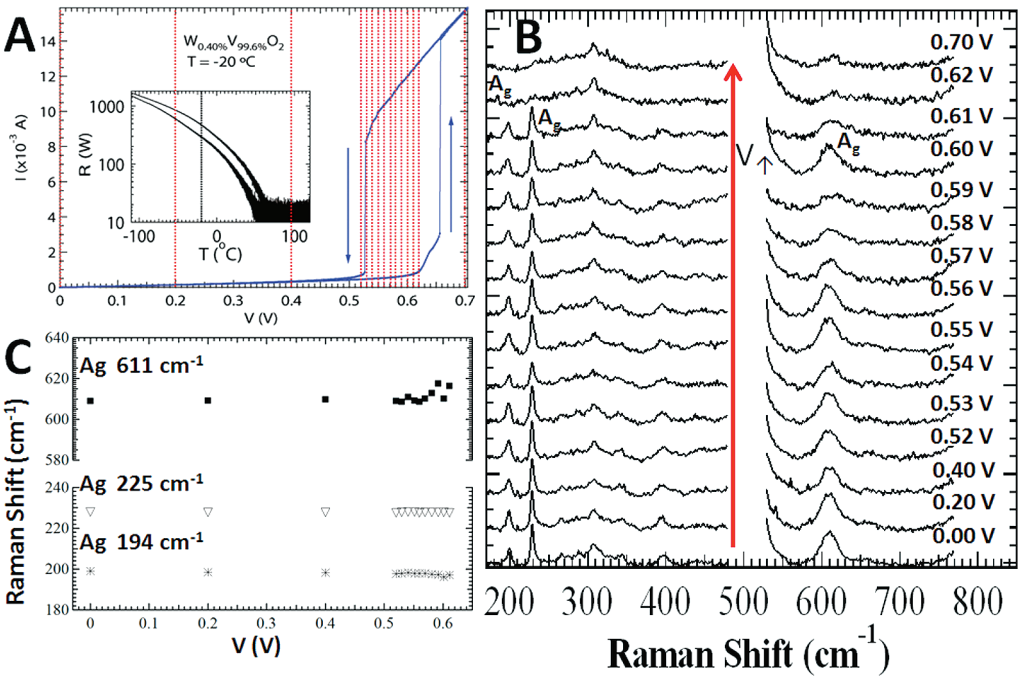

Figure 5. (A) Current *versus* voltage curve measured for a $W_xV_{1-x}O_2$ nanowire with $x \sim 0.4$ atom %. The red dotted lines indicate points at which the voltage was held constant and Raman spectra were acquired. The inset shows a plot of the resistance *versus* the temperature measured for the same exact device. (B) Raman spectra acquired for the nanowire measured in (A) at different constant voltage values. (C) Plots of the peak positions of the M1 Raman modes as a function of applied voltage.

In conclusion, solution-grown $W_xV_{1-x}O_2$ nanowires exhibit phase diagrams that are altered from undoped VO_2 and are characterized especially by stabilization of the M1 phase over M2 and T alternative ground states. Our separate *in situ* Raman spectroscopy studies of $W_xV_{1-x}O_2$ nanowires across doping-, temperature-, and voltage-induced phase transitions corroborate the idea that an M2 phase is not required to mediate the M1→R structural phase transformation. With increasing W incorporation, the nanowires are stabilized in the metallic rutile phase at room temperature, but again, no characteristic signatures of the M2 phase are noted for any of the W dopant concentrations. The absence of the M2 phase even for clamped nanowires indicates preferential stabilization of the M1 phase upon tungsten doping. Measurements of both thermal and voltage-induced transformations suggest the establishment of a coexistence regime wherein M1+R phases exist in different proportions before percolation is achieved, and the entire nanowire is transformed to a metallic R state (upon heating). Future work will focus on the application of tip-enhanced Raman spectroscopy tools to resolve discrete structural domains within the nanowires with greater spatial resolution.

METHODS

We have previously reported the synthesis of $W_xV_{1-x}O_2$ nanobelts based on the hydrothermal reduction of V_2O_5 by oxalic acid in the presence of the appropriate amount of a H_2WO_4 precursor.[16] The hydrothermal reaction was performed at 250 °C for times ranging from 12 h to 7 days. The oxalic acid concentration was carefully selected to yield phase-pure VO_2 exhibiting well-defined metal−insulator transitions in exclusion of V_6O_{13} and other substoichiometric oxides.[16] A Hitachi SU-70 scanning electron microscope operating at an accelerating voltage of 20 kV was used to acquire SEM images. A JEOL 2010 instrument operated at 200 kV was used to acquire selected area electron diffraction (SAED) patterns. To prepare the samples for HRTEM/SAED analysis, the nanostructures were dispersed in 2-propanol and then deposited onto 300 mesh carbon-coated Cu grids. The W dopant concentrations (atomic percentage of W, x in $W_xV_{1-x}O_2$) were determined using inductively coupled plasma-optical emission spectroscopy (ICP-OES). For Raman spectroscopy, nanowire samples were dispersed in 2-propanol and cast onto SiO_2, Ta, or Au substrates. The nature of the substrate had no discernible influence on the observed phase transition behavior. Raman spectra were acquired using a Jobin-Yvon Horiba Labram HR instrument coupled to an Olympus BX41 microscope using 514.5 nm laser excitation from an Ar-ion laser. An 1800 lines/mm grating was used to acquire spectra yielding a spectral resolution greater than 2 cm^{-1}. Raman spectra were acquired for 300 s intervals. The laser power was kept below 300 μW to minimize local heating. A Linkam Scientific Instruments THMS 600 thermal stage was used for the *in situ* thermal cycling experiments, and the samples were allowed to equilibrate for at least 300 s upon increasing/decreasing the temperature. For monitoring voltage-induced transitions, standard lithography followed by metallization using a substrate-cooled electron-beam evaporator was used to deposit Cr/Au electrodes onto individual nanowires dispersed on a 300 nm SiO_2/Si surface.

Acknowledgment. This work was primarily supported by the National Science Foundation under DMR 0847169. T.W. and G.S.

acknowledge support from National Science Foundation under DMR 0847324. S.B. also acknowledges support from Research Corporation for Science Advancement through a Cottrell Scholar Fellowship.

REFERENCES AND NOTES

1. Dagotto, E. Complexity in Strongly Correlated Electronic Systems. *Science* **2005**, *309*, 257–262.
2. Fulde, P.; Thalmeier, P.; Zwicknagl, G. Strongly Correlated Electrons. *Solid State Phys.* **2006**, *60*, 1–180.
3. Imada, M.; Fujimori, A.; Tokura, Y. Metal–Insulator Transitions. *Rev. Mod. Phys.* **1998**, *70*, 1039–1263.
4. Whittaker, L.; Patridge, C. J.; Banerjee, S. Microscopic and Nanoscale Perspective of the Metal–Insulator Phase Transitions of VO_2: Some New Twists to an Old Tale. *J. Phys. Chem. Lett.* **2011**, *2*, 745–758.
5. Wei, J.; Wang, Z.; Chen, W.; Cobden, D. H. New Aspects of the Metal–Insulator Transition in Single-Domain Vanadium Dioxide Nanobeams. *Nat. Nanotechnol.* **2009**, *4*, 420–424.
6. Qazilbash, M. M.; Brehm, M.; Chae, B.-G.; Ho, P.-C.; Andreev, G. O.; Kim, B.-J.; Yun, S. J.; Balatsky, A. V.; Maple, M. B.; Keilmann, F.; *et al.* Mott Transition in VO_2 Revealed by Infrared Spectroscopy and Nano-Imaging. *Science* **2007**, *318*, 1750–1753.
7. Cao, J.; Ertekin, E.; Srinivasan, V.; Fan, W.; Huang, S.; Zheng, H.; Yim, J. W. L.; Khanal, D. R.; Ogletree, D. F.; Grossman, J. C.; *et al.* Strain Engineering and One-Dimensional Organization of Metal–Insulator Domains in Single-Crystal Vanadium Dioxide Nanobeams. *Nat. Nanotechnol.* **2009**, *4*, 732–737.
8. Chudnovskiy, F.; Luryi, S.; Spivak, B. In *Future Trends in Microelectronics: The Nano Millenium*; Zaslavsky, A., Ed.; Wiley-Interscience: New York, 2002; pp 148–155.
9. Hu, B.; Ding, Y.; Chen, W.; Kulkarni, D.; Shen, Y.; Tsukruk, V. V.; Wang, Z. L. External-Strain Induced Insulating Phase Transition in VO_2 Nanobeam and Its Application as Flexible Strain Sensor. *Adv. Mater.* **2010**, *22*, 5134–5139.
10. Strelcov, E.; Lilach, Y.; Kolmakov, A. Gas Sensor Based on Metal–Insulator Transition VO_2 Nanowire Thermistor. *Nano Lett.* **2009**, *9*, 2232–2236.
11. Tselev, A.; Strelcov, E.; Luk'yanchuk, I. A.; Budai, J. D.; Tischler, J. Z.; Ivanov, I. N.; Jones, K. M.; Proksch, R.; Kalinin, S. V.; Kolmakov, A. Interplay between Ferroelastic and Metal–Insulator Phase Transitions in Strained Quasi-Two-Dimensional VO_2 Nanoplatelets. *Nano Lett.* **2010**, *10*, 2003–2011.
12. Guiton, B. S.; Gu, Q.; Prieto, A. L.; Gudiksen, M. S.; Park, H. Single-Crystalline Vanadium Dioxide Nanowires with Rectangular Cross Sections. *J. Am. Chem. Soc.* **2005**, *127*, 498–499.
13. Jones, A. C.; Berweger, S.; Wei, J.; Cobden, D. H.; Raschke, M. B. Nano-Optical Investigations of the Metal–Insulator Phase Behavior of Individual VO_2 Microcrystals. *Nano Lett.* **2010**, *10*, 1574–1581.
14. Cao, J.; Gu, Y.; Fan, W.; Chen, L. Q.; Ogletree, D. F.; Chen, K.; Tamura, N.; Kunz, M.; Barrett, C.; Seidel, J.; *et al.* Extended Mapping and Exploration of the Vanadium Dioxide Stress-Temperature Phase Diagram. *Nano Lett.* **2010**, *10*, 2667–2673.
15. Whittaker, L.; Jaye, C.; Fu, Z.; Fischer, D. A.; Banerjee, S. Depressed Phase Transition in Solution-Grown VO_2 Nanostructures. *J. Am. Chem. Soc.* **2009**, *131*, 8884–8894.
16. Whittaker, L.; Wu, T.-L.; Patridge, C. J.; Ganapathy, S.; Banerjee, S. Distinctive Finite Size Effects on the Phase Diagram and Metal–Insulator Transitions of Tungsten-Doped Vanadium(IV) Oxide. *J. Mater. Chem.* **2011**, *21*, 5580–5592.
17. Wu, T.-L.; Whittaker, L.; Banerjee, S.; Sambandamurthy, G. Temperature and Voltage Driven Tunable Metal–Insulator Transition in Individual $W_xV_{1-x}O_2$ Nanowires. *Phys. Rev. B* **2011**, *83*, 073101/1–073101/4.
18. Wu, J.; Gu, Q.; Guiton, B. S.; Leon, N.; Ouyang, L.; Park, H. Strain-Induced Self Organization of Metal–Insulator Domains in Single-Crystalline VO_2 Nanobeams. *Nano Lett.* **2006**, *6*, 2313.
19. Zhong, S.; Chou, J. Y.; Lauhon, L. J. Direct Correlation of Structural Domain Formation with the Metal Insulator Transition in a VO_2 Nanobeam. *Nano Lett.* **2009**, *9*, 4527–4532.
20. Sohn, J. I.; Joo, H. J.; Ahn, D.; Lee, H. H.; Porter, A. E.; Kim, K.; Kang, D. J.; Welland, M. E. Surface-Stress-Induced Mott Transition and Nature of Associated Spatial Phase Transition in Single Crystalline VO_2 Nanowires. *Nano Lett.* **2009**, *9*, 3392–3397.
21. Pouget, J. P.; Launois, H.; Dhaenens, J. P.; Marenda, P.; Rice, T. M. Electron Localization Induced by Uniaxial Stress in Pure VO_2. *Phys. Rev. Lett.* **1975**, *35*, 873–875.
22. Pouget, J. P.; Launois, H.; Rice, T. M.; Dernier, P.; Gossard, A.; Villeneuve, G.; Hagenmuller, P. Dimerization of a Linear Heisenberg Chain in the Insulating Phases of $V_{1-x}Cr_xO_2$. *Phys. Rev. B* **1974**, *10*, 1801–1815.
23. Ghedira, M.; Vincent, H.; Marezio, M.; Launay, J. C. Structural Aspects of the Metal–Insulator Transitions in $V_{0.985}Al_{0.015}O_2$. *J. Solid State Chem.* **1977**, *22*, 423–438.
24. Tselev, A.; Luk'yanchuk, I. A.; Ivanov, I. N.; Budai, J. D.; Tischler, J. Z.; Strelcov, E.; Kolmakov, A.; Kalinin, S. V. Symmetry Relationship and Strain-Induced Transitions between Insulating M1 and M2 and Metallic R Phases of Vanadium Dioxide. *Nano Lett.* **2010**, *10*, 4409–4416.
25. Corr, S. A.; Shoemaker, D. P.; Melot, B. C.; Seshadri, R. Real Space Investigation of Structural Changes at the Metal-Insulator Transition in VO_2. *Phys. Rev. Lett.* **2010**, *105*, 056401–056404.
26. Donev, E. U.; Lopez, R.; Feldman, L. C.; Haglund, R. F., Jr. Confocal Raman Microscopy Across the Metal–Insulator Transition of Single Vanadium Oxide Nanoparticles. *Nano Lett.* **2009**, *9*, 702–706.
27. Zhang, S.; Kim, I. S.; Lauhon, L. J. Stoichiometry Engineering of Monoclinic to Rutile Phase Transition in Suspended Vanadium Dioxide Nanobeams. *Nano Lett.* **2011**, *11*, 1443–1447.
28. Schilbe, P. Raman Scattering in VO_2. *Physica B* **2002**, *316-317*, 600–602.
29. Chou, J. Y.; Lensch-Falk, J. L.; Hemesath, E. R.; Lauhon, L. J. Vanadium Oxide Nanowire Phase and Orientation by Raman Spectroscopy. *J. Appl. Phys.* **2009**, *105*, 034310/034311–034310/034316.